Indonesian Journal of Electrical Engineering and Computer Science
Vol. 7, No. 1, July 2017, pp. 75 ~ 83
DOI: 10.11591/ijeecs.v7.i1.pp75-83

Design and Simulation of a New ZVT Bi-directional DC-DC Converter for Electric Vehicles

Rajesh Thumma*[1], Veera Venkata Subrahmanya Kumar Bhajana[2], Pramod Kumar Aylapogu[3]
School of Electronics Engineering, KIIT University, Bhubaneswar-751024, Odisha, India
Corresponding author, e-mail: rajesh.thumma88@gmail.com*[1], kumarbvvs@yahoo.co.in[2], aylapogu.pramodkumar@gmail.com[3]

Abstract

This paper presents a new zero voltage transition (ZVT) bi-directional DC-DC converter for battery back-up systems in electric vehicles. This bidirectional converter can transfer the power flow from low voltage to high voltage and vice versa. The conventional hard-switched non-isolated converter improved with the additional auxiliary cell to attain soft turn-on for the IGBTs. The main advantages of this topology are, the reduced switching stresses and better efficiancy. The main aim of this converter is to achieve the operation of zero voltage transition during the commutation of main switches from off to on by utilizing the auxiliary cell which consists of active and passive elements. The boost and buck modes of operations are achieved with the zero voltage transition which reduces the IGBTs current stresses and switching losses. This paper mainly presents the theoretical analysis of converter operation and the evaluation of the simulation results validated with the theoretical analysis.

Keywords*: ZVT, DC-DC converter, energy storage batteries, auxiliary resonant cell*

1. Introduction

Globally isolated and non isolated converters confronts a big challenge in view of low switching losses, higher switching frequency and better efficiency of the energy storage systems. Various types of PWM converters [1-2] have been implemented to decrease the conduction losses during transient states of the switching devices with the additional of integrated auxiliary cell. A non-isolated DC-DC converter [2] has obtained the zero voltage transition (ZVT) with the reduced voltage stresses, low current ripples in order to achieve the maximum power on the batteries for maximizing the battery's life. The battery energy storage systems (BESS) [4] have the functions of power conditioning and uninterruptible power supply (UPS) for interfacing bus bank and DC batteries, respectively. The class-E resonant and quasi resonant circuits [4] with single controlled switches BJT or MOSFETs are used in order to achieve a high conversion ratio (operated at higher switching frequency). There are many quasi resonant converters [5, 6] are implemented with different way of connections of passive components. However, the soft-switching operations are applied to achieve the reduced switching stresses/losses. Conventional bi-directional converters are implemented to interface small battery energy storage system with micro grid [7]. Nowadays, the renewable energy from battery storage system in electrical vehicles comes into spot light by taking into consideration of pollution effects. A non isolated DC-DC converter with PWM switching technique; it can be operated in power conditioning mode/inverter mode for the utility of power flow to load and then to charge the battery bank with automatic charging control [8]. In single phase PWM cyclo converter implemented by additional snubber circuit to get zero voltage transition (ZVT) [9]. In class-E inverter [10] and rectifier circuits, the switching losses are minimized in both step up and step down modes with the feature of soft-switching(ZVS). A high performance PWM DC-DC converter [11] with reduced EMI emissions has been achieved by controlling the *di/dt* values of switching devices. Similarly, a soft-switched non-isolated bidirectional converter [12] with auxiliary resonant circuits are utilized to obtain the zero-voltage transition/zero-current transition of the IGBTs. However, it has the drawbacks of increased additional losses and increased device count etc. In this proposed converter, the LC resonant circuits used to shape the current

Received April 12, 2017; Revised June 5, 2017; Accepted June 20, 2017

waveform at zero-voltage transition of the main semiconductor switches. A simple non-isolated boost converter [13] has been implemented with the additional H-soft-switch cell and the ZCS/ZVS operations are achieved with improved efficiency. A four port interleaved bidirectional converter [14] has the soft-switching features to the switching devices and efficient usage of photovoltaic (PV) cells are obtained with the maximum power point tracking (MPPT) control technique. A high-gain boost converter [15] has also been developed to attained the zero-voltage switching (ZVS) with additional active clamp to the main switching devices. It has reduced turn-on switching losses with improved efficiencies. However, this converter is operated at very low output power and it may not be suitable for the battery back-up systems operated under high output power. Therefore, the present work deals with the development of a new soft-switched bidirectional DC-DC converter with lower conduction losses and higher efficiency. The chief intend of this article is to design a simple ZVT bidirectional converter with improved efficiency and it can be applicable in energy storage system (super capacitors, Fuel cell, etc) of hybrid electrical vehicles. The paper mainly describes the design and simulation analysis of the proposed converter, as in the following sections II and III.

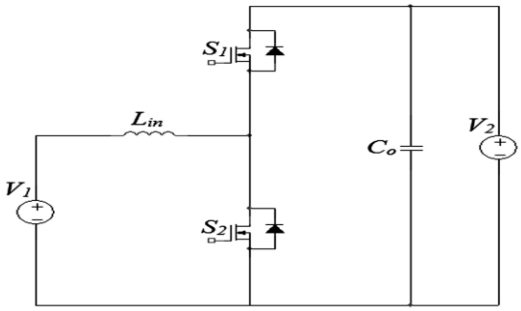

Figure 1. Hard-switched bi-directional converter

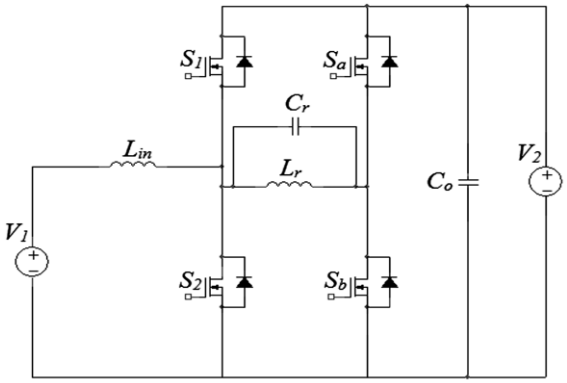

Figure 2. Proposed ZVT bi-directional buck-boost DC-DC converter

2. Circuit Description and Its Operation

The schematic diagram of the hard-switched bi-directional converter is shown in Figure 1 and proposed ZVT bidirectional DC-DC converter is shown in Figure 2. The converter comprises of two main switches (S_1, S_2), resonant inductor (L_r), resonant capacitor (C_r), input inductor and additional auxiliary switches S_a & S_b. The basic operation of this converter is in the form of boost and buck modes. However, either boost or buck mode of operation utilize only one auxiliary switch (S_a & S_b) to achieve the soft turn-on to the MOSFETs (S_1,S_2). The voltage and current waveforms of this converter are shown in Figure 3, which shows The gating signals V_{g1} represents for MOSFET S_1 in buck and V_{g2} for MOSFET S_2 in boost mode resepectively. The duty cycles chosen for S_2 ,S_b are 0.5 and 0.1 in boost mode.Similarly the gating signals used V_{ga} for MOSFET S_a and V_{gb} for MOSEFT S_b. The operating stages for the boost and buck mode are divided in to five intervals from t_0 to t_6. The current flow equivalent circuits for boost mode are shown in Figure 4(a-d) and the buck mode operations are shown in Fig.5(a,b,c,d), respectively.

2.1. Boost Mode Analysis

The boost mode operation of the proposed converter is divided into five stages with the help of principal waveforms as shown in Figure 3 and thier current flow equivalent circuits are represented in Figure 4(a-d). The boost mode operation is divided in to six intervals from t_0-t_6.

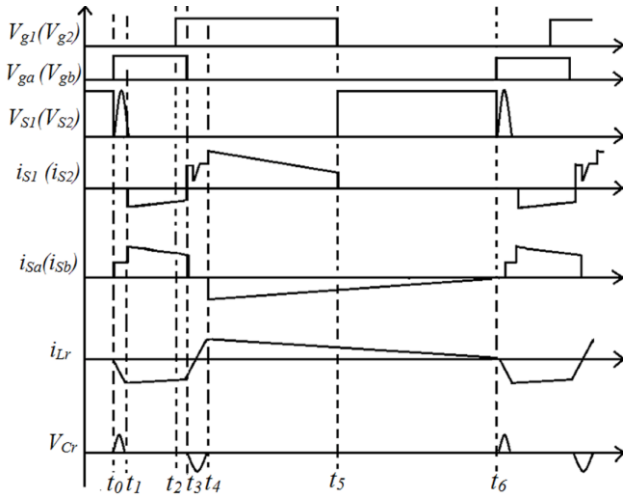

Figure 3. Principal waveforms of Buck (Boost) modes

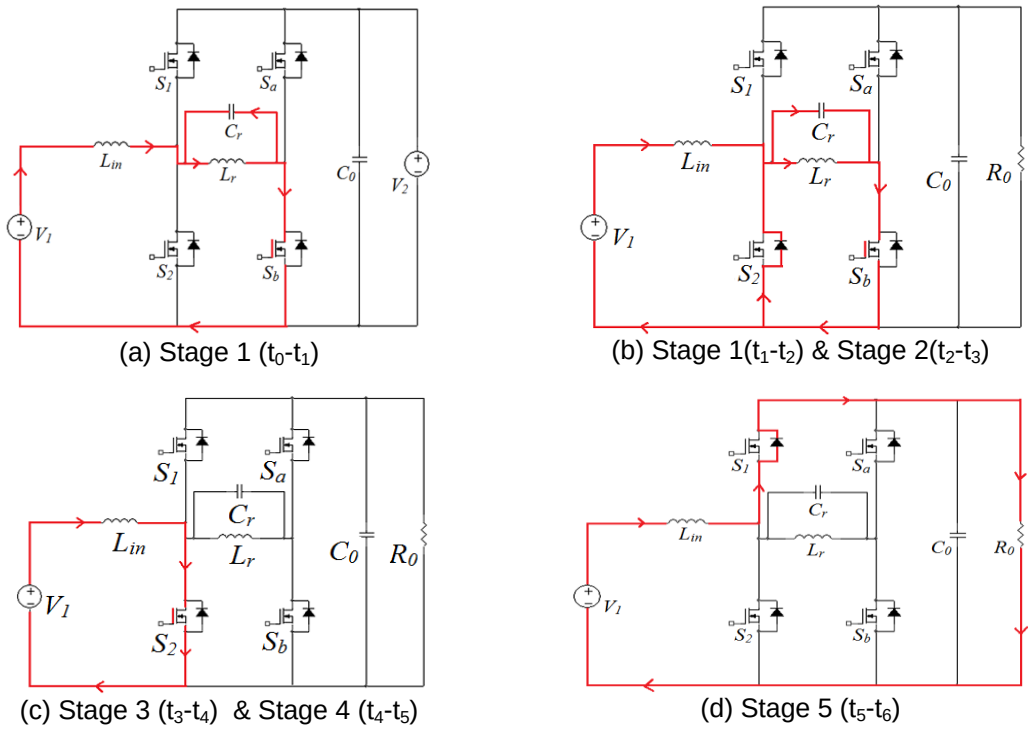

(a) Stage 1 (t_0-t_1)

(b) Stage 1(t_1-t_2) & Stage 2(t_2-t_3)

(c) Stage 3 (t_3-t_4) & Stage 4 (t_4-t_5)

(d) Stage 5 (t_5-t_6)

Figure 4. (a) Stage 1 (b) Stage 2 (c) Stage 3 & 4 (d) Stage 5: Boost mode

First Interval (t_0-t_1): At time t_0, the MOSFET S_b is turned-on to achieve the soft commutation of the main switch S_2. At this instant, the resonant inductor L_r and capacitors C_r are in resonating state. The voltage of S_2 falls in sinusoidal fashion and then becomes zero at t_1, and the resonant capacitor C_r voltage reaches zero.

Second Interval (t_1-t_2): The second interval starts at t_1, the resonant current flows through the main switch S_2 anti-parallel diode. At the end of second interval t_2, the anti-parallel diode stops conduction and its current reaches zero from negative.

Third Interval (t_2-t_3): During the third interval (t_2-t_3), the main switch S_2 is conducting and the capacitor C_r remains zero. At the end of this interval, the MOSFET S_b is turned-off.

Fourth Interval (t_3-t_4): During the fourth interval (t_3-t_4), the main switch is in conducting and voltage of C_r is being charged to the output voltage and then discharged to zero, respectively. The energy in the input inductor L_{in} accumulating via S_2. At the time t_4, the main switch is turned-off.

Fifth Interval (t_4-t_5): At time t_4, all the MOSFETs are in turned-off state, the output power transfer via L_{in}-body diode of S_1-R_0.

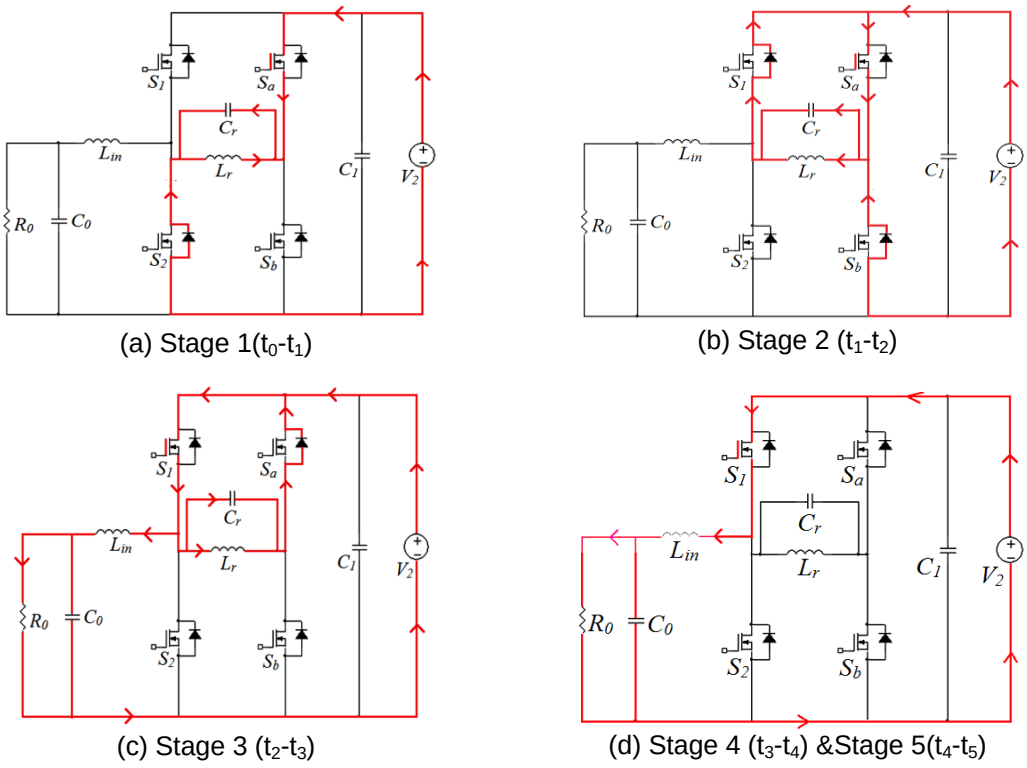

(a) Stage 1(t_0-t_1) (b) Stage 2 (t_1-t_2)

(c) Stage 3 (t_2-t_3) (d) Stage 4 (t_3-t_4) &Stage 5(t_4-t_5)

Figure 5. (a) Stage 1 (b) Stage 2 (c) Stage 3 (d) Stage 4&5: Buck mode

2.2. Buck Mode Analysis

The buck mode operation is divided into four intervals from t_0-t_4. The MOSFET S_a is turned-on at t_0, which is short-interval before S_1 gated to achieve zero-voltage transition. In the t_0-t_3 time interval, the operation of this mode is similar to the boost mode. At time t_2, the MOSFET S_1 is turned-on with zero-voltage transition operation. At time t_3, the MOSFET S_a is turned-off and S_1 is conducting and the output power is delivered through S_1 - L_{in}- R upto time t_5. From t_5-t_6, no output power will be delivered to load.

3. Theoritical Analysis

For the boost and buck mode of operations (t_0-t_1), the input inductor L_{in} and resonant inductor L_r currents are expressed as follows:

$$i_{Lin} = \frac{1}{L_{in}} \int_{t_o}^{t_1} (V_S - V_o)\, dt = \frac{1}{L_{in}} (V_S - V_o)t + I \quad (1)$$

Where V_S is source voltage in boost *(V_1)* or buck modes *(V_2) and* V_o is the output voltage.

$$i_{Lr} = \frac{1}{L_r} \int_{t_o}^{t_1} (V_o - V_s) dt = \frac{1}{Lr} (V_o - V_s)t \quad (2)$$

$$i(0) = 0 \quad i_{Lin}(t_1) = I_M \quad \text{and} \quad i_{Lr}(t_1) = I_{Lr} \tag{3}$$

$$V_{Cr}(t_1) = 0 \tag{4}$$

During the t_1-t_2 interval, the L_r, L_{in} currents and C_r voltages are expressed as follows;

$$i_{Lin} = \frac{1}{L_{in}} v_s(t) + I_{S1} \tag{5}$$

$$i_{Lr}(t_2) = I_{S1}, i_{Lr}(t_2) \approx I_{Sa} \tag{6}$$

$$V_{cr}(t) = V_0 \tag{7}$$

During the interval t_2-t_3 in boost mode stage 3, the voltage and currents of L_r and C_r are expressed as follows:

$$i_{Lin} = \frac{1}{L_{in}} V_s(t) + I_{S1} \tag{8}$$

$$i_{Lr}(t) = 0 \tag{9}$$

$$V_{cr}(t) = 0 \tag{10}$$

During the interval of time t_3-t_4, the input inductor, resonant inductor currents and resonant capacitor (C_r) voltages are expressed as given below:

$$i_{Lin} = \frac{1}{L_{in}} (V_S - V_0)t + I_{S2} \tag{11}$$

$$i_{Lr}(t) = 0 \tag{12}$$

$$V_{Cr}(t) = 0 \tag{13}$$

Similarly, the buck mode operations are also same as the boost mode. In this mode, all stages are operated with switches S_2 and S_b.

The resonant capacitor voltage V_{Cr} is equals to the ouput voltage V_o. Therefore, the characteristics are expressed as:

Impedance of the circuit is $Z = \sqrt{\frac{L_r}{C_r}} = 14.4\Omega$

Resonant angular frequency is $\omega = \frac{1}{\sqrt{L_r C_r}}$

Resonant frequency is $f_r = \frac{\omega}{2\pi} = 11.1MHz$

The resonant inductor L_r=2µH and resonant capacitor is C_r=10nF.

4. Simulation Results

The proposed converter design simulations are performed on MATLAB Simulink. The analyses of simulations are performed individually for boost and buck modes. The converter simulations were performed at 30kHz operating frequency with an input voltage of 200V and output current of 6A. The duty cycles chosen for the main switches S_1, S_2 and auxiliary switches S_a,S_b are 0.5 and 0.1, respectively. The gating signals are supplied to the switches S_2 and S_b, when this converter is operated in boost mode. During this mode, the S_2 acts as a main switch

and S_b acts as an auxiliary switch. By turning on of S_b the zero voltage transition of the main switch S_2 is achieved. Auxiliary switch is turned-on prior to gating the S_2. Figure 6 shows the source-drain voltage, current of the MOSFET S_2 and MOSFET S_b, current of L_r, voltage of capacitor C_r in boost mode. Similarly, simulations were performed for the buck mode operation with the source voltage of 400 V and output voltage of 200V. Figure 7 represents the source-drain voltage, currents of MOSFETs S_2 & S_b, L_r and capacitor voltage C_r. Figure 8 depicts the turn-on transitions of the main and auxiliary MOSFETs. The output voltage and current of the converter in boost and buck modes are represented in Figure 9 and Figure 10. The obtained output voltage and currents in boost mode are 400V and 16A respectively. Similarly 200V output voltage and 39A output currents are obtained for buck mode. In addition, Figure 11 shows the modelled converter for simulations using MATLAB. The design parameters considered for this converter are listed in Table 1. Table 2 shows the switching patterns of MOSFETS S_1,S_2, and S_a,S_b in different intervals.

Table 1. Simulation Paramters

Parameter	Symbol	Value	Unit
Input voltage	V_{in}	200	V
Output voltage	V_o	400	V
Output power	P_o	6500	W
Input inductor	L_{in}	100	µH
Resonant inductor	L_r	2	µH
Resonant capacitor	C_r	10	nF
Output capacitor	C_o	470	µF
Switching frequency	f_{sw}	30	kHz

Table 2. Switching Patterns

MOSFETs	Boost mode	Buck mode	Interval
S_1	*OFF*	ON	t_2-t_5
S_2	*ON*	OFF	t_2-t_5
S_a	*OFF*	ON	t_0-t_3
S_b	*ON*	OFF	t_0-t_3

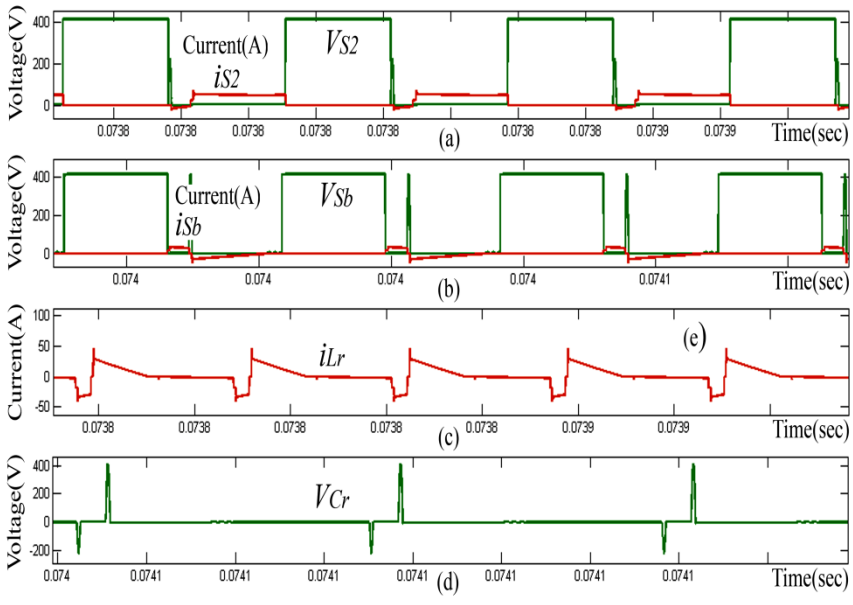

Figure 6. (a) source-drain voltage and current of S_1 (b) source-drain voltage and current of S_a(c) Resonant inductor (L_r) current (d) resonant capacitor (C_r) voltage: Boost mode

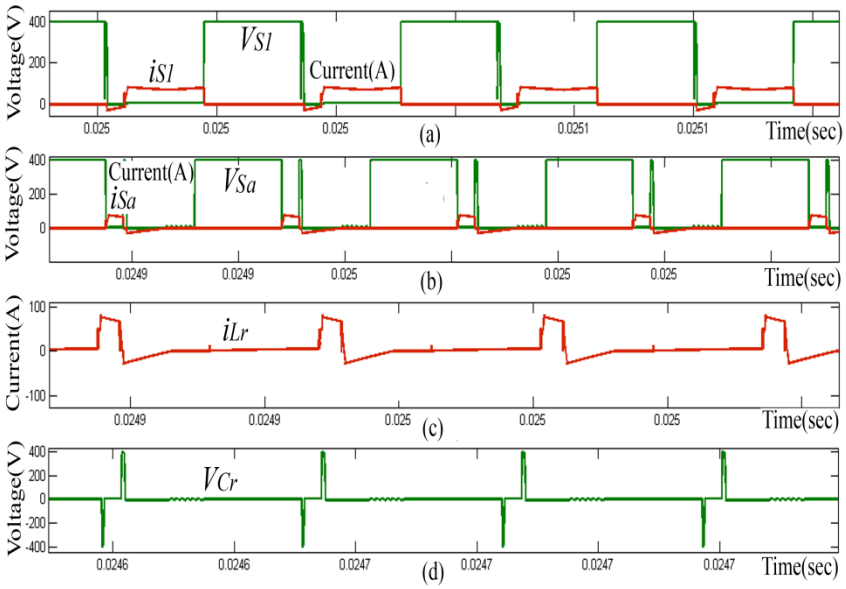

Figure 7. (a) source-drain voltage and current of S_2 (b) source-drain voltage and current of S_b (c) Resonant inductor (L_r) current (d) resonant capacitor (C_r) voltage: Buck mode

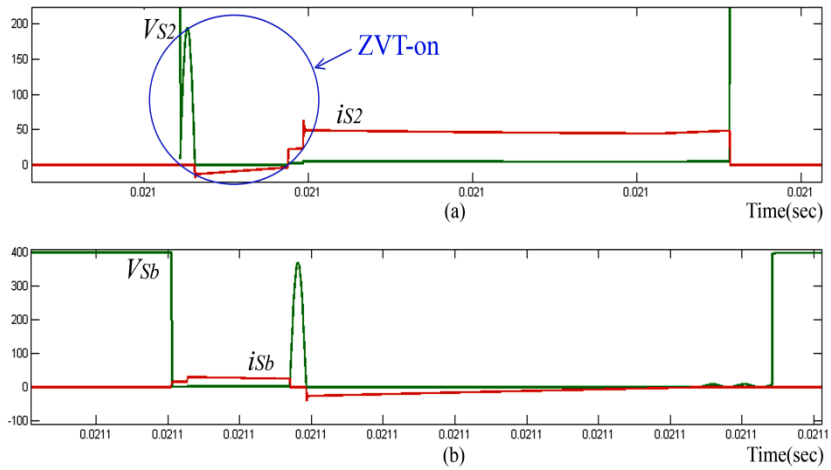

Figure 8. (a) Turn-on transition of S_2 (b) Turn-on transition of S_b

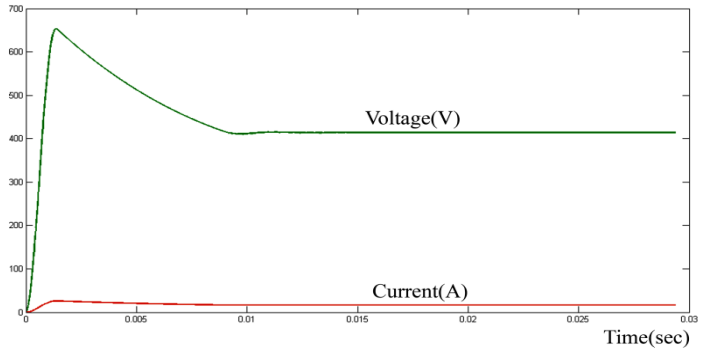

Figure 9. output voltage and current waveforms: Boost mode

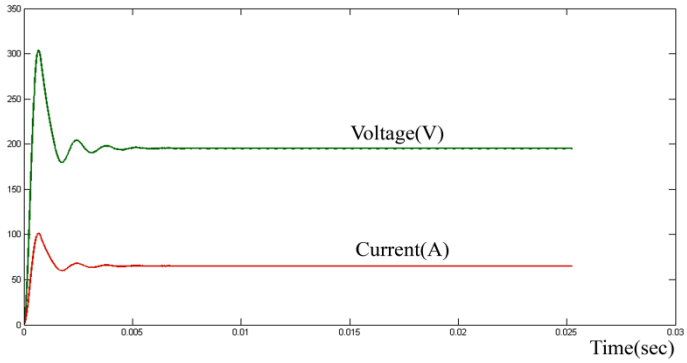

Figure 10. Output voltage and current waveforms: Buck mode

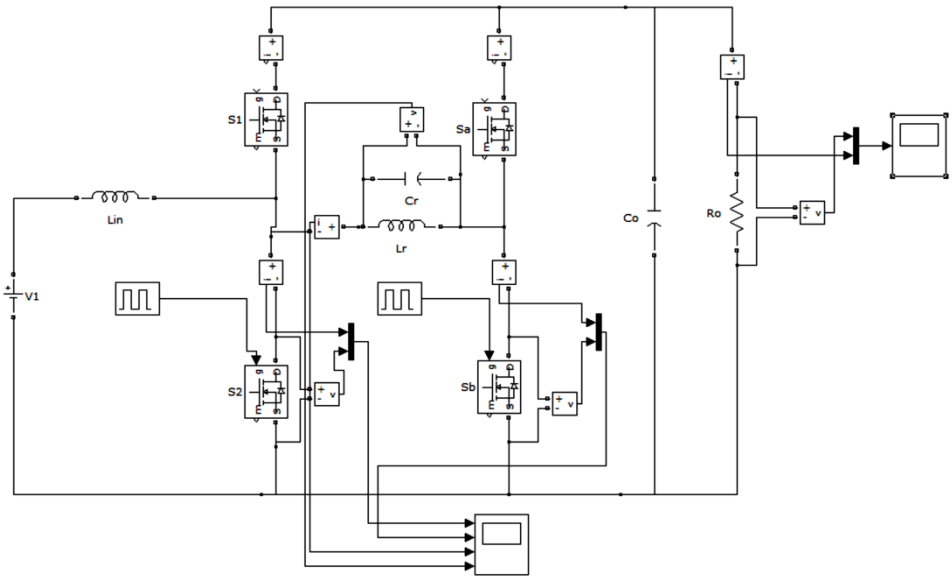

Figure 11. Simulink model of proposed converter

5. Conclusion

This article presented the design and simulation analysis of a new zero-voltage transition bi-directional DC-DC converters for battery back-up systems in hybrid electric vehicles. The main aim of this article was the simulation analysis for the design of a simple soft-switching non-isolated DC-DC converter by additional auxiliary active resonant cell. The ZVT turn-on to the main switches was achieved with reduced voltage and current stresses respectively. The design simulations performed for 100V/200V converter system under 6 kW output power. The simulated efficiencies obtained 97.5% for boost and 98.2% for buck modes, respectively. It is observed that the proposed converter has reduced turn-on switching losses and improved efficiency. The simulation results are verified with theoretical analysis.

References

[1] Dong-Yun Lee, Min-Kwang Lee, Dong-Seok Hyun, I Choy. New zero-current-transition PWM DC/DC converters without current stress. *IEEE Transactions on Power Electronics*. 2003; 18(1): 95-104.
[2] L Schuch, C Rech, HL Hey, HA Grundlinggrundling, H Pinheiro, JR Pinheiro. Analysis and Design of a New High-Efficiency Bidirectional Integrated ZVT PWM Converter for DC-Bus and Battery-Bank Interface. *IEEE Transactions on Industry Applications*. 2006; 42(5): 1321-1332.
[3] SJ Chiang, KT Chang, CY Yen. Residential photovoltaic energy storage system. *IEEE Transactions on Industrial Electronics*. 1998; 45(3): 385-394.

[4] R Redl, B Molnar, NO Sokal. *Class-E resonant regulated DC/DC power converters: analysis of operation, and experimental results at 1.5 MHZ.* IEEE Power Electronics Specialists Conference. Albuquerque, New Mexico, USA. 1983: 50-60.
[5] S Mohan, EP Cheriyan. *Bilateral converter to interface small battery energy storage system with micro-grid*. 2012 IEEE Students' Conference on Electrical, Electronics and Computer Science (SCEECS). Bhopal. 2012: 1-4.
[6] KH Liu, R Oruganti, FCY Lee. Quasi-Resonant Converters-Topologies and Characteristics. *IEEE Transactions on Power Electronics*. 1987; 2(1): 62-71.
[7] CM Liaw, TH Chen, SJ Chiang, CM Lee, CT Wang. *Small battery energy storage system*. IEE Proceedings B - Electric Power Applications. 1993; 140(1): 7-17.
[8] E Tatakis, N Polyzos. *A novel approach to evaluate the behavioral characteristics of zero-voltage switching quasi-resonant converters*. 27th Annual IEEE Power Electronics Specialists Conference. Baveno. 1996; 2: 1388-1393.
[9] A Safaee, HR Karshenas, D Yazdani, A Bakhshai, P Jain. *A novel soft-switched bidirectional single-phase PWM AC chopper with a lossless active snubber circuit*, Twenty-Sixth Annual IEEE Applied Power Electronics Conference and Exposition (APEC). Fort Worth, TX. 2011: 1106-1110.
[10] KK Saravanan, S Rajalakshmi, N Stalin, S Titus. *New Zero current transition PWM dc/dc converter without current stress.* IEEE-International Conference On Advances In Engineering, Science And Management (ICAESM -2012). Nagapattinam, Tamil Nadu. 2012: 566-570.
[11] L Schuch, C Rech, HL Hey, JR Pinheiro. Integrated ZVT auxiliary commutation circuit for input stage of double-conversion UPSs. *IEEE Transactions on Power Electronics*. 2004; 19(6): 1486-1497.
[12] AP Kumar, VVSK Bhajana, P Drabek. *A novel ZVT/ZCT bidirectional DC-DC converter for energy storage applications*. International Symposium on Power Electronics, Electrical Drives, Automation and Motion (SPEEDAM). Capri, Italy. 2016: 979-983.
[13] A Elamathy, G Vijayagowri, V Nivetha. Bidirectional Battery Charger for PV Using Interleaved Fourport DC-DC Converter. *TELKOMNIKA Indonesian Journal of Electrical Engineering.* 2015; 14(3): 428-433.
[14] AlirezaKaviani-Arani, Alireza Gheiratmand. Soft Switching Boost Converter Solution for Increase the Efficiency of Solar Energy Systems. *TELKOMNIKA Indonesian Journal of Electrical Engineering.* 2015; 13(3): 449-457.
[15] Aiswarya TM, M Prabhakar. An Efficient High Gain DC-DC Converter for Automotive Applications. *International Journal of Power Electronics and Drive System (IJPEDS).* 2015; 6(2): 242-252.